Journal of Physics and Its Applications

Journal homepage : https://ejournal2.undip.ac.id/index.php/jpa/index

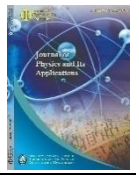

Electron contamination for 6 MV photon beams from an Elekta linac: Monte Carlo simulation

Choirul Anam[1], Djarwani S Soejoko[2], Freddy Haryanto[3], Sitti Yani[4], and Geoff Dougherty[5]

[1]*Department of Physics, Faculty of Sciences and Mathematics, Diponegoro University, Jl. Prof. Soedarto SH, Tembalang, Semarang 50275, Central Java, Indonesia. anam@fisika.fsm.undip.ac.id*
[2]*Department of Physics, Faculty of Mathematics and Natural Sciences, University of Indonesia, Depok, West Java, Indonesia*
[3]*Department of Physics, Faculty of Mathematics and Natural Sciences, Bandung Institute of Technology, Ganesha 10, Bandung 40132, West Java, Indonesia*
[4]*Department of Physics, Faculty of Mathematics and Natural Sciences, Insitut Pertanian Bogor (IPB University), Jl. Meranti, Kampus IPB Dramag Bogor 16680, West Java, Indonesia*
[5] *Department of Applied Physics and Medical Imaging, California State University Channel Islands, Camarillo, CA 93012, USA*

ARTICLE INFO

Article history:
Received : 2 May 2020
Accepted : 28 May 2020
Available online : 10 June 2020

Keywords:
Monte Carlo simulation
Elekta linear accelerator
Electron contamination

ABSTRACT

This study investigates electron contamination for 6 MV photon beams from an Elekta linear accelerator (linac) using Monte Carlo simulation. The linac head was simulated by the BEAMnrc code and the absorbed dose in a phantom was calculated using the DOSXYZnrc code. The parameters of the initial electron beams on the target, such as mean energy and radial intensity distribution, were determined by matching the calculated dose distributions with the measured dose (at 10 x 10 cm^2 field size and 90 cm source-skin distance). The central axis depth-dose curves of electron contamination were calculated for various field sizes from 5 x 5 cm^2 to 40 x 40 cm^2. We investigated the components that generated the electron contamination for a field size of 10 x 10 cm^2. The optimal initial electron beam energy was 6.3 MeV with a full-width half maximum (FWHM) of the radial intensity distribution of 1.0 mm. These parameters were found to be in good agreement with the measured data. Electron contamination increased as the field size increased. At a depth of 1.0 mm and field sizes of 5 x 5, 10 x 10, 20 x 20, 30 x 30, and 40 x 40 cm^2, the doses from electron contamination were 3.71, 5.19, 14.39, 18.97 and 20.89 %, respectively. Electron contamination decreased with increased depth. At a depth of 15 mm, the electron contamination was about 1 %. It was mainly generated in the air column between the linac head and the phantom (3.65 %), the mirror (0.99 %), and the flattening filter (0.59 %) (for a depth of 1.0 mm and field size of 10 x 10 cm^2).

1. Introduction

Radiotherapy is an essential modality in cancer treatment. Radiotherapy employs ionizing radiation and its interaction with tissue can activate cell death, either directly or indirectly [1-4]. The radio-sensitivity of most cancer cells is higher than healthy cells. Thus, ionizing radiation can kill cancer cells while maintaining as many healthy cells as possible. The ionizing radiation is carefully planned at the specific direction, energy, field size and intensity to achieve a maximum and homogeneous dose in the cancer tumor, while surrounding healthy tissue receives the minimum possible dose [3,4].

In general, the radiation beam used in radiotherapy comprises either electrons or photons. Electron beams are produced by a linear accelerator (linac) machine, while photon radiation can be generated by either a Cobalt-60 (Co-60) machine or by a linac machine [5-9]. Electron beams are usually used for tumors located at or near the surface of the skin (superficial tumors), while photon beams are used for tumors located at a greater depth [3].

Photon beams from radiotherapy units (Co-60 or linac), in fact, are no longer pure photon beams, but a mixture of photons and a small amount of electrons produced by the photon beams [10]. This effect is known as electron contamination [4]. The electron contamination has been studied by numerous authors [11-16]. Various techniques were used to determine the amount of electron contamination [7], including direct measurement using electron filter plates and sweeping magnets to remove electrons, analytical methods, and Monte Carlo simulation. However, no studies have been conducted on the parts and components that produce the electron contamination. The electron contaminations increase skin and subcutaneous tissue doses, however it does not have an impact to the clinical target volume (CTV) [17-20]. It is important to note that it is impossible to remove all electron contaminations. If the characteristics of the

electron contaminations and the components producing it are well-understood, then the electron contaminations can be minimized [4, 16]. In this study, the sources of electron contaminations are investigated using Monte Carlo simulation.

2. Methodology

2.1. Linac head and phantom

We investigated electron contamination by Monte Carlo simulation using the EGSnrc code. The EGSnrc code consisted of the BEAMnrc for linac head simulation [21] and the DOSXYZnrc for calculation of absorbed dose in the phantom [22]. For all steps of the simulations, an electron cut-off energy (AE) of 0.521 MeV and photon cut-off energy (AP) of 0.01 MeV were chosen. The number of initial electrons on the target to produce x-ray beams was taken to be 3 x 10^8 and the skin-source distance (SSD) was 90 cm.

All components of the linac head were specified exactly from an Elekta SL Series Linac Physics Manual. The components of the linac head were target, target block, primary collimator, flattening filter, monitor chamber, mirror, and jaws (Fig. 1). The phantom was simulated using the DOSXYZnrc code. The phantom was made from water, and had dimensions of 40 cm x 40 cm x 40 cm. The dose zones for percentage depth dose (PDD) were determined along the central axis. Determination of the build-up dose was performed in the same way as the PDD determination, except it was focused on the region between the surface and the maximum depth dose (d_m) and used smaller voxels. The dose zones for the lateral profile were perpendicular to the central axis. It was measured at a depth of 1.5 cm.

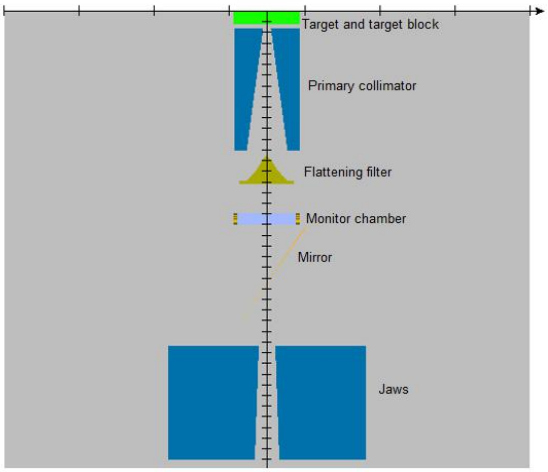

Fig 1: Components of the Elekta linac head: target, target block, primary collimator, flattening filter, monitor chamber, mirror, and jaws.

To determine the optimum model, the energies of initial electrons were varied from 5.7 to 6.6 MeV. The full-width half maximums (FWHMs) of radial intensity distribution of incident electrons were varied from 0.5 to 2 mm. After an optimum model was achieved, i.e. in the good agreement with the measured data [23], the model was used for the next simulation.

2.2. Dose of electron contaminations

The dose of electron contamination was determined by investigating electrons from the phase space file (PSF) produced by the BEAMnrc code. The source of electron contamination was traced by the LATCH (program code to trace particle's history). Number LATCH for Target, Target Block, Primary Collimator, Flattening Filter, Monitor Chamber, Mirror, Jaws and the air between linac head and phantom, were 1, 2, 3, 4, 5, 6, 7, and 8, respectively.

3. Results and Discussions

3.1. Standard model determination

Before calculation of electron contamination, it is important to accurately determine a standard model of the initial electron beams, in terms of energy and radial distribution of incident electrons. The energy and the FWHM of their radial intensity distribution of incident electrons were varied [24]. The resulting maximum depth dose, PDD, and the dose profile were compared with those obtained from direct measurements.

Fig. 2(a) shows that the maximum depth dose (d_m) increased as the energy of incident electron increased. The maximum depth dose is 1.5 cm for electron energies of 5.7 and 6.0 MeV, 1.6 cm for an energy of 6.3 MeV, and 1.7 cm for an energy of 6.6 MeV. The measurement of maximum depth dose was at a depth of 1.5 cm. Figure 2(b) shows that the dose profiles from measurement and simulations coincide with each other, and that variations of energy contribute only a little to the dose profile. In the Monte Carlo simulation, the incident electron energy was chosen as 6.3 MeV for the standard model, because at this value the maximum depth dose, PDD and dose profile are in best agreement with the results of direct measurement.

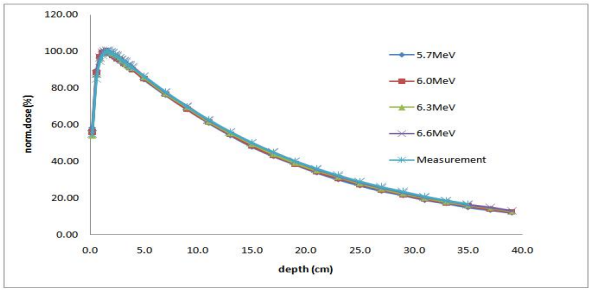

(a)

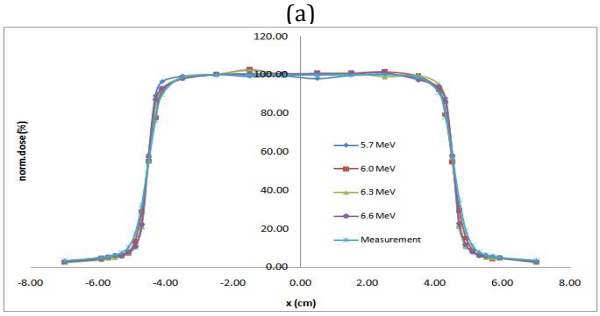

(b)

Fig. 2: (a) Curves of PDDs, and (b) dose profiles at depth of 1.5 cm from measurement and simulations for various electron energies. The FWHM of radial intensity was 1.0 mm, and field size was 10 x 10 cm^2.

There are two factors to determine standard model of FWHM, i.e. PDD and dose profile. Figure 3 shows that the PDDs and dose profiles from measurement and simulation for various FWHMs are very similar. However, a FWHM of 1.0 mm is in best agreement with measurement data. In addition,

Elekta also recommends this value [25]. This value is recommended to ensure that the X-ray source is small enough to reduce the effect of penumbra.

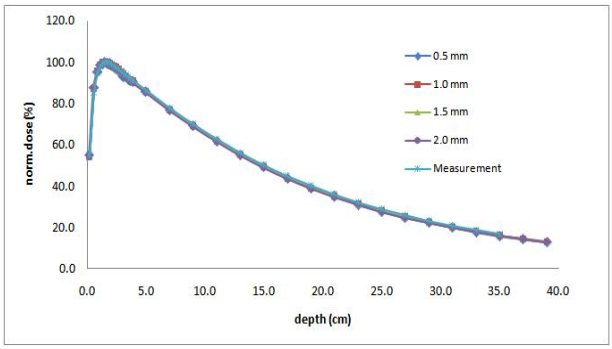

(a)

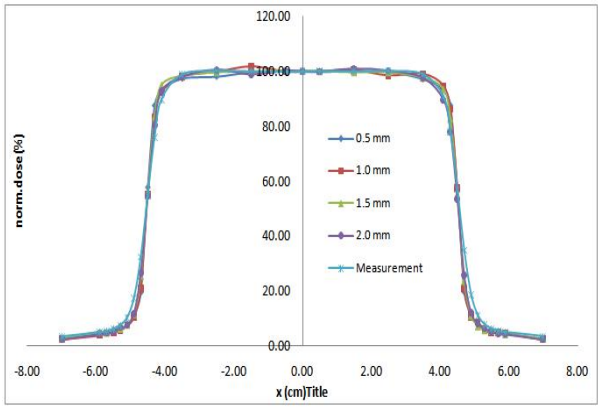

(b)

Fig. 3: (a) Curves of PDDs, and (b) dose profiles at a depth of 1.5 cm from measurement and simulations for various FWHMs of 0.5, 1.0, 1.5, and 2.0 mm. The energy of initial electron beams was 6.3 MeV, and field size was 10 x 10 cm^2.

3.2. Electron contamination

Figure 4(a) shows the doses at the build-up region for a field size of 10 x 10 cm^2. The photon doses increase with increased depth. Doses in build-up region increase due to secondary charged particles (electrons and positrons) that are released in the phantom by photon interactions (i.e. photoelectric effect, Compton effect, and pair production). The charge particles have relatively long range and then deposit their energy kinetic in the phantom.

Figure 4(b) shows that the doses of electron contamination decreased with depth. Decreasing electron contamination dose is due to a decreasing energy of electron contaminations in their tracks. It is shown from Figure 4(b) that the doses of electron contaminations are about 1.0% at a depth 1.5 cm (i.e. depth of dose maximum (d_m)). An increase of field size causes an increase of electron contamination at the surface or beneath the surface of the phantom [16]. At a depth of 1.0 mm, the doses of electron contaminations were 3.71, 5.19, 14.39, 18.97, and 20.89 % for field sizes of 5 x 5, 10 x 10, 20 x 20, 30 x 30, and 40 x 40 cm^2, respectively. These findings are in agreement with previous studies [3, 24]. It is shows that the energy of electron contaminations at field sizes from 5 x 5 to 40 x 40 cm^2 were similar, but the number of contaminating electrons varies with field size.

In Monte Carlo simulation, the probability of every interaction can be followed and the source of electron contamination can be traced. The electron contamination generated from the various components of the linac head can be found using Figure 5. The electron contamination is mainly generated in the air column between the linac head and the phantom, mirror and flattening filter. The other parts of the linac head do not contribute much.

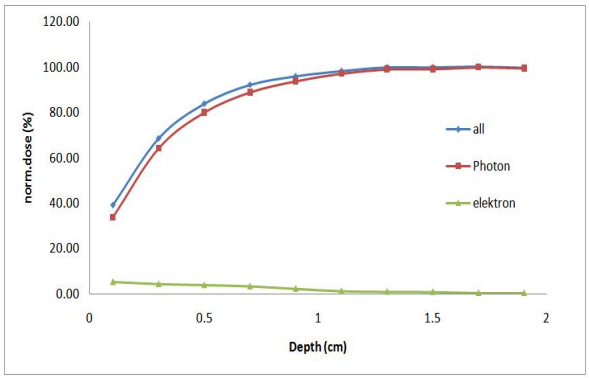

(a)

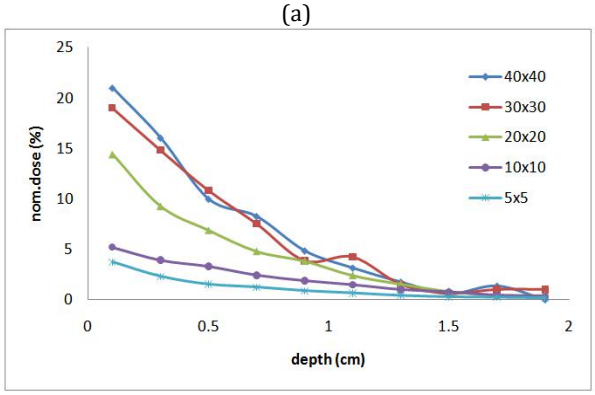

(b)

Fig. 4: (a) Curves of doses at the build-up region for field size of 10 x 10 cm^2, and (b) The doses of electron contamination for various field sizes. The energy of initial electron beams was 6.3 MeV, and the FWHM of radial intensity was 1.0 mm.

The fluctuation of percent doses at a field sizes of 30 x 30 and 40 x 40 cm^2 due to the random nature of small number of electron contaminations. If the simulation used greater number of particles, then greater number electron contaminations will be produced and the fluctuation of electron contaminations will be reduced. However, it needs additional computation time.

The electron contamination generated in the air column between the linac head and the phantom was very significant [26], due to the large volume of the air column and its position near the water phantom. The electron contamination generated in the mirror is also significant because all photon beams interact with the mirror, and there are no materials between mirror and phantom except the air. Although the mirror is very thin (consisting of mylar with a thickness of 0.3 mm), it provides a significant contribution to the electron contamination.

The contribution from flattening filter is smaller than that from the mirror, because most of its generated electrons are absorbed within the flattening filter itself.

The monitor chamber contributes insignificant electron contamination, because it is very thin and made from mylar film, plates and air. The primary collimator and jaws also give a small contribution,

because the interaction with the photon beams occur only at the edge of the beam [17]. And the contribution of the primary collimator is insignificant because there are many components that absorb electron contamination generated within it.

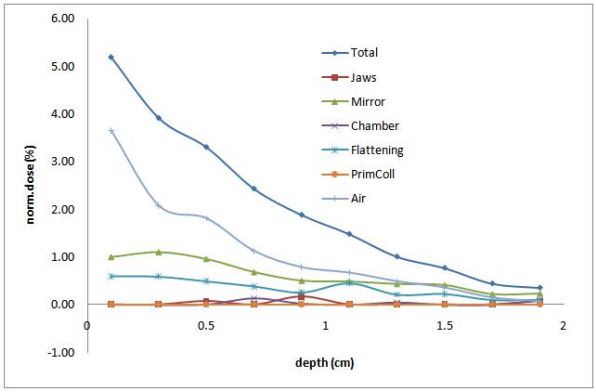

Fig. 5: Electron contaminations generated from various components of the linac head and air between the linac head and phantom for field size of 10 x10 cm^2.

4. Conclusions

The dose due to electron contamination and their sources have been investigated. It is important to determine a standard model before performing Monte Carlo simulation. The standard initial electron beam parameters for the model were 6.3 MeV energy and 1.0 mm FWHM of the radial intensity distribution. These values were found to be in best agreement with the measured data. The electron contamination increased as the field size increased, and the dose from electron contamination dropped off rapidly with depth. At a depth of 1.5 cm, the contribution of electron contaminations is about 1%. These contaminations are generated mainly in the air column between the linac head and the phantom, as well as in the mirror and the flattening filter.

Acknowledgment

The research was funded by the Program Penelitian Kolaborasi Indonesia (PPKI), World Class University Program, 2020.

Conflict of interest

The authors declare that they have no conflict of interest.

References

1. F. N. Ihya, C. Anam, and V. Gunawan, "Pembuatan kurva isodosis 2D dengan menggunakan kurva percentage depth dose (PDD) dan profil dosis dengan variasi kedalaman untuk treatment planning system," Berkala Fisika **16** 131-138 (2013)
2. D. T. Nugraheni, V. Gunawan, and C. Anam, "Prediction of 2D isodose curve on arbitrary field size in radiation treatment palnning system (RTPS)," Jurnal Sains dan Matematika **23** 7-13 (2015)
3. P. Metcalfe, T. Kron, and P. Hoban, "The physics of radiotheraphy X-rays and electrons," Madison, Wisconsin: Med. Phys. Publishing (2007)
4. P. M. K. Leung, "The physical basis of radiotherapy," Canada: The Ontario Cancer Institute incorporating The Princess Margareth Hospital (1990)
5. N. D. Prasetyo, W. Setiabudi, and C. Anam, "Analisis perubahan kurva percentage depth dose (PDD) dan dose profile untuk radiasi foton 6MV pada fantom thoraks," Jurnal Sains dan Matematika **20** 103-108 (2012)
6. N. F. Nuzula, K. Adi, and C. Anam, "Correction of 2D isodose curve on the sloping surface using tissue air ratio (TAR) method," Jurnal Sains dan Matematika **23** 65-71 (2015)
7. A. Rizani, W. S. Budi, and C. Anam, "Simulasi Monte Carlo untuk menentukan dosis sinar-X 6 MV pada ketakhomogenan medium jaringan tubuh," Berkala Fisika **15** 49 – 56 (2012)
8. C. Anam, "Kajian spektrum sinar-X 6 MV menggunakan simulasi Monte Carlo," Berkala Fisika **14** 49- 54 (2011)
9. C. Anam, "Development of 2D isodose curve from the PDD and dose profiles using Matlab," Proceeding of ISNPINSA 48-52 (2012)
10. S. Yani, I. G. E. Dirgayussa, M. F. Rhani, R. C. X. Soh, F. Haryanto, and I. Arif, "Monte Carlo study on electron contamination and output factors of small field dosimetry in 6 MV photon beam," Smart Science **4** 1-8 (2016)
11. T. C. Zhu and J. R. Palta, "Electron contamination in 8 and 18 MV photon beams," Med. Phys. **25** 12–19 (1998)
12. G. Malataras, C. Kappas, and D. M. J. Lovelock, "A Monte Carlo approach to electron contamination sources in the Saturne-25 and -41," Phys. Med. Biol. **46** 2435–2446 (2001)
13. W. Vander Zee and J. Welleweerd, "Calculating photon beam characteristics with Monte Carlo techniques," Med. Phys. **26** 1883–1892 (1999)
14. M. K. Fix, M. Stampanoni, P. Manser, E. J. Born, R. Mini, and P. Ruegsegger, "A multiple source model for 6MV photon beam dose calculations using Monte Carlo," Phys. Med. Biol. **46** 1407–1427 (2001)
15. G. X. Ding, "Energy spectra, angular spread, fluence profiles and dose distributions of 6 and 18 MV photon beams: Results of Monte Carlo simulations for a Varian 2100 EX accelerator," Phys. Med. Biol. **47** 1025–1046 (2002)
16. Y. Indra, "Electron contaminant in 6 MV X-rays beams," Jakarta: University of Indonesia Thesis, (2006)
17. F. Seif and M. R., "Evaluation of electron contamination in cancer treatment with megavoltage photon beams: Monte Carlo study," J. Biomed. Phys. Eng. **5** 31-38 (2015)

18. N. Kucuk, A. Kilic, G. Kemikler, L. Ozkan, and K. Engin, “Analyses of surface dose from high energy photon beams for different clinical setup parameters,” Turk J. Med. Sci. **32** 211–215 (2002)
19. A. Lopez Medina, A. Teijeiro, J. Garcia, J. Esperon, J. A. Terron, D. P. Ruiz, et al., “Characterization of electron contamination in megavoltage photon beams,” Med. Phys. **32** 1281–1292 (2005)
20. B. Nilsson and A. Brahme, “Electron contamination from photon beam collimators,” Radiother Oncol **5** 235-244 (1986)
21. D. W. O. Rogers, C. M. Ma, B. Walters, G. X. Ding, D. Sheikh-Bagheri, and G. Zhang, “BEAMnrc users manual,” NRCC Report PIRS-0509(A)revF, Canada: National Research Council of Canada (2001)
22. B. R. B. Walters and D.W.O. Rogers, “DOSXYZnrc users manual,” Technical Report PIRS–794. Ottawa, Canada: National Research Council of Canada (2002)
23. F. Haryanto, M. Fippel, W. Laub, O. Dohm, and F. Nusslin, “Investigation of photon beam output factors for conformal radiation therapy—Monte Carlo simulations and measurements,” Phys. Med. Biol. **47** N133–N143 (2002)
24. K. Aljarrah, G. C. Sharp, T. Neicu, and S. B. Jiang, “Determination of the initial beam parameters in Monte Carlo linac simulation,” Med. Phys. **33** 850-858 (2006)
25. Elekta, Elekta SL series linac physics manual
26. F. Verhaegen and J. Seuntjens, “Monte Carlo modeling of external radiotherapy photon beams,” Phys. Med. Biol. **48** R107–R164 (2003)